Chem Biol Drug Des 2016; **87:** 361–373

Research Article

Synthesis, *In vitro* and Docking Studies of New Flavone Ethers as α-Glucosidase Inhibitors

Syahrul Imran[1,2], Muhammad Taha[1,2,*], Nor Hadiani Ismail[1,2,*], Syed Muhammad Kashif[3], Fazal Rahim[4], Waqas Jamil[3], Habibah Wahab[5] and Khalid Mohammed Khan[6]

[1]*Atta-ur-Rahman Institute for Natural Product Discovery, Universiti Teknologi MARA, Puncak Alam Campus, Selangor, DE 42300, Malaysia*
[2]*Faculty of Applied Sciences, Universiti Teknologi MARA, Shah Alam, Selangor, DE 40450, Malaysia*
[3]*Institute of Advance Research Studies in Chemical Sciences, University of Sindh, 76080 Jamshoro, Pakistan*
[4]*Department of Chemistry, Hazara University, 21300 Mansehra, Pakistan*
[5]*Pharmaceutical Design and Simulation Laboratory, School of Pharmaceutical Sciences, Universiti Sains Malaysia, 11800 Pulau Pinang, Malaysia*
[6]*H. E. J. Research Institute of Chemistry, International Center for Chemical and Biological Sciences, University of Karachi, Karachi 75270, Pakistan*
**Corresponding authors: Muhammad Taha, taha_hej@yahoo.com and muhamm9000@puncakalam.uitm.edu.my; Nor Hadiani Ismail, norhadiani@puncakalam.uitm.edu.my*

We report herein the synthesis, α-glucosidase inhibition and docking studies for a series of 3–15 new flavones. A simple nucleophilic substitution reaction takes place between 3′hydroxyflavone (2) with halides to afford the new flavones. Chalcone (1), 3′hydroxyflavone (2) and the newly synthesized flavones (3–15) were being evaluated for their ability to inhibit activity of α-glucosidase. Compounds 2, 3, 5, 7–10 and 13 showed good inhibitory activity with IC_{50} values ranging between 1.26 and 36.44 μM as compared to acarbose (IC_{50} = 38.25 ± 0.12 μM). Compounds 5 (5.45 ± 0.08 μM), 7 (1.26 ± 0.01 μM) and 8 (8.66 ± 0.08 μM) showed excellent inhibitory activity, and this may be due to trifluoromethyl substitution that is common for these compounds. Compound 7, a 2,5-trifluoromethyl-substituted compound, recorded the highest inhibition activity, and it is thirty times better than the standard drug. Docking studies for compound 7 suggest that both trifluoromethyl substituents are well positioned in a binding pocket surrounded by Phe300, Phe177, Phe157, Ala278, Asp68, Tyr71 and Asp214. The ability of compound 7 to interact with Tyr71 and Phe177 is extremely significant as they are found to be important for substrates recognition by α-glucosidase.

Key words: docking, enzyme inhibition, ether linkage, flavone, α-glucosidase

Received 29 June 2015, revised 24 August 2015 and accepted for publication 7 September 2015

Diabetes mellitus is a serious worldwide chronic metabolic disorder resulting from carbohydrate metabolism (1–3). This lifestyle-related disease is characterized by increase in blood glucose concentration (hyperglycaemia), and it results in numerous complications such as cardiovascular, retinopathy, nephropathy and neuropathy diseases (4). The trend displayed that number of diabetes mellitus patients increases from 153 to 347 million between the year 1980 and 2008 (5). Findings by The International Diabetes Federation in 2011 showed that about 366 million people have diabetes and expected to increase by up to 552 million by 2030 (6). This is supported by projection of World Health Organization (WHO) projection, which predicts diabetes to become the seventh leading cause of death worldwide by 2030 (7). Type II diabetes mellitus that is common in developed countries is characterized by impaired insulin secretion and reduced insulin sensitivity (8–12). One of the ways to reduce type II diabetes mellitus is by suppressing absorption and digestion of dietary carbohydrates. This can be achieved by inhibiting digestive enzymes, such as α-glucosidase and α-amylase (13).

α-Glucosidase (EC3.2.1.20) is an enzyme commonly found in small intestine. α-Glucosidase hydrolyses carbohydrates to produce glucose during food digestion. Glucose produced is being absorbed into blood stream, thus increases postprandial blood glucose level and leads to diabetes. Considered as an important and attractive drug target, inhibiting α-glucosidase can be effective in treating type II diabetes mellitus, which reduces and controls postprandial blood glucose spike (14–18). They retard glucose produced through hydrolysis of α-(1-4)-linked *D*-glucose residues from the non-reducing end of α-glucoside (19). This reduces the rate of glucose absorption and, therefore, decreases plasma glucose level. α-Glucosidase inhibition has attracted plenty of attention from pharmaceutical industry as a treatment method of diseases such as diabetics, viral infections, hepatitis and cancer (20–22). In addition to preventing diabetes, controlled glucose level in blood may prevent

 doi: 10.1111/cbdd.12666

obesity, hyperlipoproteinaemia and hyperlipidaemia (23). Inhibitors for α-glucosidase function by reversibly inhibit digestive α-glucosidase. Inhibitors for α-glucosidase are found to show antitumor, antidiabetic, antiviral and immunoregulatory activities (24–26). Research on α-glucosidase inhibitors such as castanospermine, *N*-butyl-deoxynojirimycin and deoxynojirimycin showed that they are potent against HIV replication (27). α-Glucosidase also enables monosaccharide removal from viral glycoproteins; thus, its inhibitors can alter cell-to-cell signalling, virus recognition by the cell, and can be used in the treatment of viral diseases, cancer and immune regulations (28–32).

Flavone is one of the classes of flavonoids that is present in fruits and vegetables. Flavones are being consumed in daily diet, and they improve health without giving any major side effect (33). Identifying new synthetic methods to synthesize and structurally modify flavone now considered important goals in exploring diverse roles of flavones. Thus, naturally obtained flavones having a variety of biological activities can be used as lead compound for synthesis of semi- and purely synthetic flavone derivatives. Flavone scaffold is an important structure found in many pharmaceutically active compounds. They are structurally diverse and possess a variety of biological activity. This reason has increased the interest of medicinal chemists to further study flavones as lead molecules to treat various diseases. Recently, researchers had focused a lot on flavones bioactivities such as free radicals scavenging ability and protection against peroxidation of lipid (34,35). Researchers also showed interest in some flavonoids due to their ability to modulate NADPH oxidase activity and endothelial nitric oxide metabolism (36–42). It has been established that flavonoids such as kaempferol, luteolin, apigenin, chrysin and baicalein have the capability of inhibiting α-glucosidase activity (43,44), taking into consideration of the importance of ring A, B and C towards the inhibition of α-glucosidase activity. Shin *et al.* (45) have shown that a series of alkyl or acetyl derivatives of chrysin have hypoglycaemic effects.

In this research, flavone derivatives having ether linkage were synthesized and evaluated for their yeast α-glucosidase inhibitory activity. We attempted to study the effect of various substituents at different position on the inhibitory effect in terms of how these compounds molecularly bind towards α-glucosidase protein. This will enable us to identify new inhibitors and structural features contributing towards α-glucosidase activity inhibition.

Experimental

Chemistry

Melting points were determined using Sinosource SGW X-4 melting point apparatus with microscope (Guangzhou, China). IR spectra obtained using PerkinElmer Spectrum 100 FTIR Spectrometer (Waltham, MA, USA). NMR spectroscopy was obtained using Bruker Ultra Shield FT NMR 500 MHz and Avance III 600 Ascend spectrometer (Wissembourg, France). EI-MS spectroscopic analysis had been obtained using Finnigan-MAT-311-A instrument (Bremen, Germany). Thin-layer chromatography (TLC) was performed using precoated silica gel plates (Merck, Darmstadt, Germany, Kieselgel 60F-254, 0.20 mm).

Synthesis of (E)-1-(2-hydroxyphenyl)-3-(3-hydroxyphenyl)prop-2-en-1-one (1)

In a 250-mL flask, 2′-hydroxyacetophenone (30 mmol) was being mixed with 3-hydroxybenzaldehyde (30 mmol). The mixture was dissolved in 50 mL of 15% (w/v) sodium hydroxide in ethanol and stirred at room temperature. Reaction progress was monitored using TLC, and upon completion, diluted sulphuric acid was added to allow precipitation. The precipitate was filtered and crystallized in ethanol to afford pure product. Orange crystal; yield 84%; ^{1}H NMR (500 MHz, DMSO-d_6) δ 12.45 (s, 1H), 9.68 (s, 1H), 8.23 (d, J = 8.1 Hz, 1H), 7.94 (d, J = 15.5 Hz, 1H), 7.75 (d, J = 15.5 Hz, 1H), 7.57 (s, 1H), 7.34 (d, J = 7.6 Hz, 1H), 7.29 (d, J = 7.9 Hz, 1H), 7.26 (s, 1H), 7.01 (dd, J = 7.8, 4.1 Hz, 2H), 6.91 (dd, J = 4.5, 3.4 Hz, 1H); ^{13}C-NMR (125 MHz, DMSO-d_6): δ 193.25, 161.64, 157.14, 143.95, 137.86, 135.68, 130.73, 128.84, 122.57, 122.21, 120.59, 119.75, 119.41, 117.60, 114.85; HREI-MS: m/z calcd for $C_{15}H_{12}O_3$ [M]+ 240.0786; found 240.0784; Anal. Calcd for $C_{15}H_{12}O_3$: C, 74.99; H, 5.03; found: C, 75.01; H, 5.05.

Synthesis of 2-(3-hydroxyphenyl)-4H-chromen-4-one (2)

Compound **1** (22.4 mmol) was mixed with iodine (0.23 mmol). The mixture was dissolved in 50 mL of DMSO and refluxed at 170 °C. After 3 h, sodium thiosulphate was added to the reaction mixture followed by excessive amount of water to allow precipitation. The product was rinsed and allowed to dry at room temperature to afford pure product. Light orange solid; yield 90%; ^{1}H-NMR (500 MHz, DMSO-d_6): δ 9.86 (s, 1H), 8.07 (dd, J = 7.9, 1.7 Hz, 1H), 7.85 (ddd, J = 8.6, 7.1, 1.7 Hz, 1H), 7.78 (dd, J = 8.4, 0.6 Hz, 1H), 7.56 – 7.48 (m, 2H), 7.45 (t, J = 2.1 Hz, 1H), 7.39 (t, J = 7.9 Hz, 1H), 7.02 (dd, J = 8.1, 2.4 Hz, 1H), 6.92 (s, 1H); ^{13}C-NMR (125 MHz, DMSO-d_6): δ 191.5, 161.0, 157.4, 140.3, 136.2, 129.6, 126.3, 121.4, 120.7, 118.0, 117.0, 115.3, 113.4, 78.7, 43.5; HREI-MS: m/z calcd for $C_{15}H_{10}O_3$ [M]+ 238.0630; found 238.0627; Anal. Calcd for $C_{15}H_{10}O_3$: C, 75.61; H, 4.23; found: C, 75.62; H, 4.24.

General procedure for synthesis of flavone ethers (3–15)

Compound **4** (1.0 mmol) and benzyl halides (1.0 mmol) were being mixed with potassium carbonate (1.0 mmol) in a 50-mL round-bottom flask. The mixture was being

dissolved in 20 mL of acetone and refluxed. Progress monitored using TLC, and upon completion, solvent was being removed using rotary evaporator. Product was collected and rinsed with diethyl ether to afford pure product.

2-(3-((4-nitrobenzyl)oxy)phenyl)-4H-chromen-4-one (3)

Light yellow solid; yield 76%; ^{1}H-NMR (500 MHz, DMSO-d_6): δ 7.87 (t, J = 8.4 Hz, 1H), 7.84 (d, J = 8.4 Hz, 1H), 7.73 (d, J = 8.2 Hz, 2H), 7.70 (d, J = 7.2 Hz, 2H), 7.61 (d, J = 8.2 Hz, 2H), 7.48 (t, J = 7.7 Hz, 2H), 7.39 (t, J = 7.4 Hz, 1H), 7.30 (dd, J = 8.1, 2.3 Hz, 1H), 7.13 (s, 1H), 5.31 (s, 2H); ^{13}C-NMR (125 MHz, DMSO-d_6): δ 178.28, 163.27, 158.69, 156.48, 147.98, 144.72, 135.38, 134.07, 128.96, 128.39, 128.39, 126.34, 125.47, 125.23, 123.42, 123.42, 119.53, 118.39, 118.21, 115.14, 105.97, 70.94; HREI-MS: m/z calcd for $C_{22}H_{15}NO_5$ [M]+ 373.0950; found 373.0953; Anal. Calcd for $C_{22}H_{15}NO_5$: C, 70.77; H, 4.05; N, 3.75; found: C, 70.76; H, 4.05; N, 3.77.

2-(3-(benzyloxy)phenyl)-4H-chromen-4-one (4)

White solid; yield 81%; ^{1}H-NMR (600 MHz, DMSO-d_6): δ 8.30 (d, J = 8.4 Hz, 2H), 8.07 (d, J = 7.9 Hz, 1H), 7.86 (d, J = 7.2 Hz, 1H), 7.83 (d, J = 8.3 Hz, 1H), 7.79 (d, J = 8.6 Hz, 3H), 7.75 (d, J = 7.8 Hz, 1H), 7.53 (dd, J = 14.5, 7.2 Hz, 2H), 7.30 (d, J = 7.9 Hz, 1H), 7.12 (s, 1H), 5.44 (s, 2H); ^{13}C-NMR (125 MHz, DMSO-d_6): δ 178.13, 163.35, 158.62, 156.38, 137.18, 135.32, 133.98, 128.95, 128.51, 128.51, 128.37, 128.37, 128.16, 126.29, 125.63, 125.19, 119.43, 118.34, 118.53, 115.44, 105.97, 70.94; HREI-MS: m/z calcd for $C_{22}H_{16}O_3$ [M]+ 328.1099; found 328.1103; Anal. Calcd for $C_{22}H_{16}O_3$: C, 80.47; H, 4.91; found: C, 80.46; H, 4.92.

2-(3-((3-(trifluoromethyl)benzyl)oxy)phenyl)-4H-chromen-4-one (5)

Light yellow solid; yield 88%; ^{1}H-NMR (500 MHz, DMSO-d_6): δ 8.05 (dd, J = 8.0, 1.5 Hz, 1H), 7.89 (s, 1H), 7.82–7.86 (m, 3H), 7.78 (t, J = 1.5 Hz, 1H), 7.73 (t, J = 8.0 Hz, 2H), 7.69 (d, J = 7.5 Hz, 1H), 7.54 (d, J = 8.0 Hz, 1H), 7.52 (d, J = 6.0 Hz, 1H), 7.30 (dd, J = 8.0, 2.5 Hz, 1H), 7.10 (s, 1H), 5.37 (s, 2H); ^{13}C-NMR (125 MHz, DMSO-d_6): δ 178.28, 163.27, 158.56, 156.18, 139.35, 135.53, 133.73, 132.52, 132.28, 128.73, 128.26, 126.44, 125.63, 125.37, 125.14, 124.85 (d, J = 262.15 Hz), 124.09, 119.58, 118.35, 118.33, 115.54, 105.73, 71.33. HREI-MS: m/z calcd for $C_{23}H_{15}F_3O_3$ [M]+ 396.0973; found 396.0976; Anal. Calcd for $C_{23}H_{15}F_3O_3$: C, 69.70; H, 3.81; found: C, 69.72; H, 3.79.

2-(3-((4-(tert-butyl)benzyl)oxy)phenyl)-4H-chromen-4-one (6)

Light orange solid; yield 74%; ^{1}H-NMR (500 MHz, DMSO-d_6): δ 8.06 (d, J = 7.5 Hz, 1H), 7.83–7.86 (m, 2H), 7.73 (s, 1H), 7.70 (d, J = 8.0 Hz, 1H), 7.49–7.54 (m, 2H), 7.44 (s, 4H), 7.25 (dd, J = 8.0, 2.0 Hz, 1H), 7.10 (s, 1H), 5.20 (s, 2H), 1.29 (s, 9H); ^{13}C-NMR (125 MHz, DMSO-d_6): δ 179.41, 163.24, 158.65, 156.27, 150.31, 137.26, 135.30, 134.02, 129.91, 127.62, 127.62, 126.14, 125.68, 125.47, 125.47, 125.31, 119.38, 118.39, 118.24, 115.14, 105.63, 70.74, 34.39, 31.93, 31.93, 31.93; HREI-MS: m/z calcd for $C_{26}H_{24}O_3$ [M]+ 384.1725; found 384.1729; Anal. Calcd for $C_{26}H_{24}O_3$: C, 81.22; H, 6.29; found: C, 81.23; H, 6.31.

2-(3-((2,5-bis(trifluoromethyl)benzyl)oxy)phenyl)-4H-chromen-4-one (7)

Yellowish white solid; yield 92%; ^{1}H-NMR (500 MHz, DMSO-d_6): δ 8.24 (s, 1H), 8.07–8.10 (m, 2H), 8.02 (s, 1H), 7.86 (d, J = 7.0 Hz, 1H), 7.79–7.82 (m, 2H), 7.78 (d, J = 8.0 Hz, 1H), 7.56 (d, J = 8.0 Hz, 1H), 7.53 (d, J = 8.0 Hz, 1H), 7.31 (dd, J = 8.0, 2.5 Hz, 1H), 7.13 (s, 1H), 5.47 (s, 2H); ^{13}C-NMR (125 MHz, DMSO-d_6): δ 178.19, 163.27, 158.86, 156.38, 140.46, 136.43, 135.72, 135.59, 133.82, 128.94, 128.37, 126.74, 126.46, 125.91, 125.37, 125.23, 123.86, 123.13, 119.68, 118.47, 118.13, 115.54, 105.63, 69.35; HREI-MS: m/z calcd for $C_{24}H_{14}F_6O_3$ [M]+ 464.0847; found 464.0852; Anal. Calcd for $C_{24}H_{14}F_6O_3$: C, 62.08; H, 3.04; found: C, 62.09; H, 3.02.

2-(3-((3-((trifluoromethyl)thio)benzyl)oxy)phenyl)-4H-chromen-4-one (8)

White solid; yield 76%; ^{1}H-NMR (500 MHz, DMSO-d_6): δ .07 (dd, J = 7.9, 1.3 Hz, 1H), 7.85 (dd, J = 6.9, 1.6 Hz, 1H), 7.82 (dd, J = 8.4, 0.8 Hz, 1H), 7.79 (d, J = 8.1 Hz, 2H), 7.77–7.75 (t, J = 2.0 Hz, 1H), 7.73 (d, J = 7.8 Hz, 1H), 7.68 (d, J = 8.4 Hz, 2H), 7.53 (td, J = 8.0, 4.5 Hz, 2H), 7.29 (dd, J = 7.9, 2.8 Hz, 1H), 7.10 (s, 1H), 5.35 (s, 2H); ^{13}C-NMR (125 MHz, DMSO-d_6): δ 178.12, 163.35, 158.69, 156.28, 144.39, 139.26, 135.33, 133.53, 130.47, 130.24, 128.96, 126.34, 126.23, 125.47, 125.15, 124.64, 123.36 (d, J = 261.5 Hz), 119.68, 118.57, 118.36, 115.34, 105.91, 71.43; HREI-MS: m/z calcd for $C_{23}H_{15}F_3O_3S$ [M]+ 428.0694; found 428.0697; Anal. Calcd for $C_{23}H_{15}F_3O_3S$: C, 64.48; H, 3.53; found: C, 64.46; H, 3.51.

4-((3-(4-oxo-4H-chromen-2-yl)phenoxy)methyl) benzonitrile (9)

Light red solid; yield 83%; ^{1}H-NMR (500 MHz, DMSO-d_6): δ 8.07 (d, J = 7.8 Hz, 1H), 7.90 (d, J = 8.0 Hz, 2H), 7.86 (t, J = 7.2 Hz, 1H), 7.83 (t, J = 8.9 Hz, 1H), 7.77–7.69 (m, 4H), 7.62–7.49 (m, 2H), 7.28 (dd, J = 8.2, 2.5 Hz, 1H), 7.10 (s, 1H), 5.38 (s, 2H); ^{13}C-NMR (125 MHz, DMSO-d_6): δ 178.32, 163.24, 158.68, 156.38, 144.36, 135.37, 133.91, 130.75, 130.75, 128.82, 127.41, 127.41, 126.14, 125.47, 125.38, 119.43, 119.09, 118.28, 118.39, 115.14, 112.29, 105.83, 70.74; HREI-MS: m/z calcd for $C_{23}H_{15}NO_3$ [M]+ 353.1052; found 353.1055; Anal. Calcd

for $C_{23}H_{15}NO_3$: C, 78.17; H, 4.28; N, 3.96; found: C, 78.18; H, 4.26; N, 3.95.

2-(3-((4-methoxybenzyl)oxy)phenyl)-4H-chromen-4-one (10)

Brown solid; yield 85%; ^{1}H-NMR (500 MHz, DMSO-d_6): δ 8.07 (d, J = 7.9 Hz, 1H), 7.86–7.80 (m, 2H), 7.75–7.67 (m, 2H), 7.51 (d, J = 7.8 Hz, 2H), 7.44 (d, J = 8.6 Hz, 2H), 7.25 (dd, J = 8.2, 2.4 Hz, 1H), 7.08 (s, 1H), 6.98 (d, J = 8.6 Hz, 2H), 5.16 (s, 2H), 3.77 (s, 3H); ^{13}C-NMR (125 MHz, DMSO-d_6): δ 178.25, 163.98, 160.12, 158.76, 156.54, 135.24, 133.83, 130.63, 129.12, 128.81, 126.54, 125.73, 125.28, 119.47, 118.33, 118.25, 115.34, 113.41, 105.92, 70.74, 56.13; HREI-MS: m/z calcd for $C_{23}H_{18}O_4$ [M]+ 358.1205; found 358.1201; Anal. Calcd for $C_{23}H_{18}O_4$: C, 77.08; H, 5.06; found: C, 77.06; H, 5.07.

2-(3-(2-oxo-2-(pyren-1-yl)ethoxy)phenyl)-4H-chromen-4-one (11)

Dark yellow solid; yield 94%; ^{1}H-NMR (600 MHz, DMSO-d_6): δ 8.89 (d, J = 9.4 Hz, 1H), 8.78 (d, J = 7.9 Hz, 1H), 8.47 (d, J = 7.8 Hz, 1H), 8.44 (d, J = 7.2 Hz, 1H), 8.35–8.42 (m, 2H), 8.31 (d, J = 8.4 Hz, 1H), 8.26 (d, J = 9.0 Hz, 1H), 8.18 (d, J = 7.8 Hz, 2H), 8.05 (d, J = 7.9 Hz, 1H), 7.77 (s, 1H), 7.74 (t, J = 8.1 Hz, 1H), 7.68 (d, J = 8.4 Hz, 1H), 7.54 (t, J = 8.0 Hz, 1H), 7.49 (t, J = 7.5 Hz, 1H), 7.33 (dd, J = 8.3, 2.3 Hz, 1H), 7.13 (s, 1H), 5.94 (s, 2H); ^{13}C-NMR (125 MHz, DMSO-d_6): δ 201.46, 178.28, 163.29, 158.48, 156.21, 135.86, 135.23, 135.46, 133.98, 131.87, 131.74, 131.74, 131.44, 128.71, 128.65, 128.29, 127.89, 127.62, 127.37, 127.37, 127.28, 126.34, 125.53, 125.31, 125.24, 125.02, 122.87, 119.58, 118.38, 118.11, 115.34, 105.97, 73.64; HREI-MS: m/z calcd for $C_{33}H_{20}O_4$ [M]+ 480.1362; found 480.1359; Anal. Calcd for $C_{33}H_{20}O_4$: C, 82.49; H, 4.20; found: C, 82.47; H, 4.22.

2-(3-(allyloxy)phenyl)-4H-chromen-4-one (12)

Dark orange solid; yield 87%; ^{1}H-NMR (600 MHz, DMSO-d_6): δ 8.07 (dd, J = 7.9, 1.1 Hz, 1H), 7.86 (dd, J = 6.7, 1.6 Hz, 1H), 7.84 (d, J = 0.9 Hz, 1H), 7.71 (d, J = 7.8 Hz, 1H), 7.67 (t, J = 1.5 Hz, 1H), 7.56–7.48 (m, 3H), 7.21 (dd, J = 8.2, 1.9 Hz, 1H), 7.11 (s, 1H), 5.47 (d, J = 18.9 Hz, 1H), 5.31 (d, J = 12.1 Hz, 1H), 4.72 (d, J = 5.3 Hz, 2H); ^{13}C-NMR (125 MHz, DMSO-d_6): δ 178.24, 163.38, 158.72, 156.38, 134.56, 134.45, 133.94, 129.20, 126.44, 125.47, 125.14, 119.27, 118.42, 118.25, 117.42, 115.15, 105.97, 70.15; HREI-MS: m/z calcd for $C_{18}H_{14}O_3$ [M]+ 480.1362; found 480.1359; Anal. Calcd for $C_{18}H_{14}O_3$: C, 77.68; H, 5.07; found: C, 77.70; H, 5.08.

2-(3-((2,3-difluorobenzyl)oxy)phenyl)-4H-chromen-4-one (13)

Dark orange solid; Yield 68%; ^{1}H-NMR (500 MHz, DMSO-d_6): δ 8.07 (d, J = 7.8 Hz, 1H), 7.86 (dd, J = 6.7, 1.6 Hz, 1H), 7.83 (d, J = 8.2 Hz, 1H), 7.79 (t, J = 1.5 Hz, 1H), 7.75 (d, J = 7.8 Hz, 1H), 7.53 (d, J = 7.9 Hz, 2H), 7.48 (d, J = 8.5 Hz, 1H), 7.45 (d, J = 6.2 Hz, 1H), 7.30 (dd, J = 8.6, 2.3 Hz, 2H), 7.14 (s, 1H), 5.35 (s, 2H); ^{13}C-NMR (125 MHz, DMSO-d_6): δ 177.68, 163.35, 158.76, 156.26, 152.81, 151.53, 135.93, 133.53, 130.24, 128.43, 126.91, 125.53, 125.28, 125.05, 124.46, 119.58, 118.47, 118.28, 116.76, 115.29, 105.97, 69.22; HREI-MS: m/z calcd for $C_{22}H_{14}F_2O_3$ [M]+ 364.0911; found 364.0908; Anal. Calcd for $C_{22}H_{14}F_2O_3$: C, 72.52; H, 3.87; found: C, 72.50; H, 3.88.

2-(3-((3-methylbenzyl)oxy)phenyl)-4*H*-chromen-4-one (14)

Light orange solid; yield 71%; ^{1}H-NMR (500 MHz, DMSO-d_6): δ 8.07 (d, J = 7.8 Hz, 2H), 8.02 (d, J = 8.2 Hz, 1H), 7.87–7.84 (m, 2H), 7.83 (s, 1H), 7.74 (s, 1H), 7.71 (d, J = 7.8 Hz, 1H), 7.54–7.50 (m, 3H), 7.21 (s, 1H), 7.11 (s, 1H), 5.20 (s, 2H), 2.34 (s, 3H); ^{13}C-NMR (125 MHz, DMSO-d_6): δ 178.29, 163.21, 158.72, 156.38, 136.91, 136.74, 135.43, 133.97, 128.81, 128.30, 128.44, 127.32, 126.64, 126.34, 125.42, 125.19, 119.58, 118.69, 118.43, 115.14, 105.90, 71.58, 21.27; HREI-MS: m/z calcd for $C_{23}H_{18}O_3$ [M]+ 342.1256; found 342.1253; Anal. Calcd for $C_{23}H_{18}O_3$: C, 80.68; H, 5.30; found: C, 80.69; H, 5.28.

3-((3-(4-oxo-4*H*-chromen-2-yl)phenoxy)methyl) benzonitrile (15)

Brown solid; yield 79%; ^{1}H-NMR (500 MHz, DMSO-d_6): δ 8.06 (d, J = 7.0 Hz, 1H), 8.01 (d, J = 7.0 Hz, 1H), 7.88–7.81 (m, 4H), 7.76 (s, 1H), 7.73 (d, J = 7.9 Hz, 1H), 7.65 (t, J = 7.8 Hz, 1H), 7.56–7.49 (m, 2H), 7.29 (dd, J = 8.2, 2.4 Hz, 1H), 7.11 (s, 1H), 5.31 (s, 2H); ^{13}C-NMR (125 MHz, DMSO-d_6): δ 178.24, 163.35, 158.76, 156.38, 140.21, 135.63, 134.07, 132.82, 131.45, 130.19, 128.82, 127.83, 126.28, 125.53, 125.38, 119.58, 119.14, 118.42, 118.16, 115.31, 110.65, 105.97, 71.59; HREI-MS: m/z calcd for $C_{23}H_{15}NO_3$ [M]+ 353.1052; found 353.1047; Anal. Calcd for $C_{23}H_{15}NO_3$: C, 78.17; H, 4.28; N, 3.96; found: C, 78.18; H, 4.26; N, 3.97.

α-Glucosidase inhibition assay

The α-glucosidase inhibition assay had been carried out using baker's yeast α-glucosidase (EC 3.2.1.20) and *p*-nitrophenyl-α-D-glucopyranoside (46–50). The samples (5 μg/mL) were prepared by dissolving the compounds **1**–**15** in DMSO. Test samples (10 μL) which had been prepared were reconstituted in 100 μL of phosphate buffer (100 mM) at pH 6.8 in 96-well microplate and incubated with 50 μL of baker's yeast α-glucosidase for 5 min before 50 μL of *p*-nitrophenyl-α-D-glucopyranoside (5 mM) was added. After incubating for 5 min, the absorbance was measured at 405 nm using SpectraMax plus384 (Molecular Devices Corporation, Sunnyvale, CA, USA). Blank in which the substrate was changed with 50 μL of buffer

was analysed to accurately determine the background absorbance. Control sample was prepared to contain 10 μL DMSO instead of test samples. Percentage of enzyme inhibition was measured using the following formula:

$$\%\,\text{inhibition} = [(A - B)/A] \times 100$$

where [A] represents absorbance of control samples and [B] corresponds to absorbance in the presence of test samples.

Homology modelling

Homology model for *Saccharomyces cerevisiae* α-glucosidase was built using crystal structure of α-D-glucose bound isomaltase from Saccharomyces cerevisiae (PDB ID: 3A4A) which shares 72% identical and 85% similar sequence with α-glucosidase. Protein sequence for Baker's yeast α-glucosidase (MAL12) was obtained from UniProt (http://www.uniprot.org). Sequence alignment and homology modelling were performed using SWISS-MODEL, which is a fully automated homology modelling pipeline SWISS-MODEL, managed by Swiss Institute of Bioinformatics (51–53).

Docking studies

The structure of all compounds was prepared using Chem3D by CambridgeSoft (Waltham, MA, USA). The geometry and energy of the structures were being optimized using Steepest-Descent and Polak-Ribiere algorithm in HyperChem. AUTODOCK 4.2 (54) was used to identify the binding modes of flavone derivatives (**1**–**15**) responsible for the activity. Protein file (pdb) was being further optimized by removing water molecules and adding hydrogen atoms. The docking grid box was set at 40 × 40 × 40 with a spacing value of 0.375 Å. Genetic algorithm (GA) with default settings was employed for the studies. In the search parameter, number of runs was set at 100, while the other settings were left as default. The docking results had been visualized using DISCOVERY STUDIO VISUALIZER 3.5a 2012. and PYMOLb.

Results and Discussion

Chemistry

Flavone ethers **3**–**15** had been synthesized through pathways in Schemes 1 and 2. 2-(3-Hydroxyphenyl)-4*H*-chromen-4-one (**2**) which is the key intermediate for the synthesis of target compounds (**3**–**15**) was prepared through three steps. In Scheme 1, 2′-hydroxyacetophenone undergoes aldol condensation with 3-hydrobenzaldehyde in ethanolic-potassium hydroxide to form (*E*)-1-(2-hydroxyphenyl)-3-(3-hydroxyphenyl)prop-2-en-1-one (**1**). Chalcone **1** was then cyclized into flavone **2** through oxidative cyclization using iodine as the oxidizing agent. Flavone ethers **3**–**15** were synthesized through a single-step reaction of 3′-hydroxyflavone (**2**) with various halides, in the presence of potassium carbonate as base catalyst (Scheme 2).

All the newly synthesized compounds were confirmed by the various analytical techniques (^{1}H-NMR, ^{13}C-NMR, MS and elemental analysis). All spectral data were in accordance with assumed structures (Table 1).

In vitro α-glucosidase inhibition

In continuation of our study on enzyme inhibition activity (48,55–58), compounds **1**–**15** had been and evaluated for their α-glucosidase inhibition activity. The assay had been carried out using baker's yeast α-glucosidase (EC 3.2.1.20). The result in Table 2 showed that compounds synthesized inhibit α-glucosidase activity with IC_{50} values that range between 1.26 and 88.66 μM. Comparison

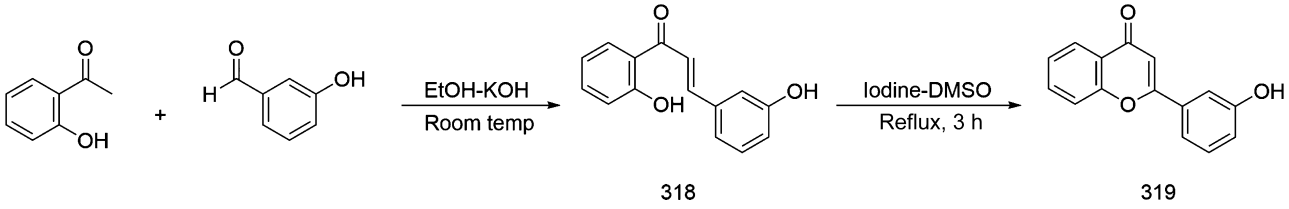

Scheme 1: Synthesis of 3′-hydroxyflavone **2**.

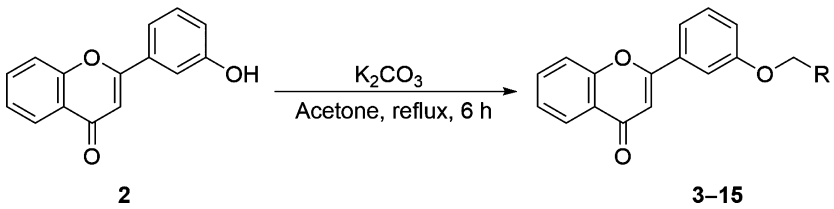

Scheme 2: Synthesis of flavone ethers **3**–**15**.

Table 1: Novel flavone ethers **3**–**15** that were synthesized and tested for α-glucosidase inhibition activity

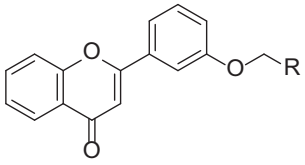

3-15

Compound	R	Compound	R
3	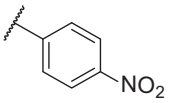	**10**	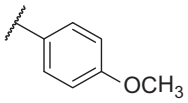
4	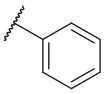	**11**	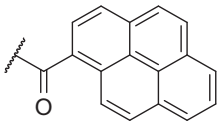
5	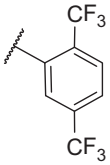	**12**	
6	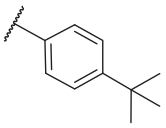	**13**	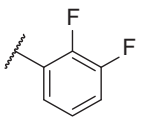
7	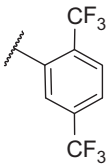	**14**	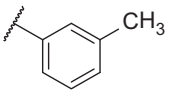
8	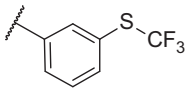	**15**	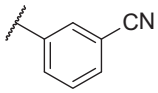
9	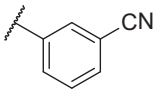		

between results for chalcone **1** and flavone **2** clearly shows that flavone **2** has better activity as compared to chalcone **1**. This indicates that cyclization and introduction of ring B have somehow affected the activity and increases the inhibition activity.

Among the compounds that are showing good inhibition activity as compared to acarbose are compounds **2**, **3**, **5**, **7**, **8**, **9**, **10** and **13**. Compounds having fluorine substituents such as compounds **5**, **7**, **8** and **13** are showing excellent inhibitory activity. Compound **7**, which is a 2,5-trifluoromethyl-substituted compound, recorded the highest inhibition activity for this series. Compound **7** has an IC_{50} value of 1.26 ± 0.01 μM, and it is thirty times better than the standard drug. Further analysis on the results showed that compound **5**, which has a trifluoromethyl substituent at *meta* position, is less active than compound **7**. Compound **5** has an IC_{50} value of 5.45 ± 0.08 μM and is lacking one trifluoromethyl substituent as compared to compound **7**. Other compounds that are weakly active

Table 2: α-Glucosidase inhibitory activity by flavone ethers **1**–**15**

Compound	IC_{50} (μM ± SEM)	Compound	IC_{50} (μM ± SEM)
1	44.66 ± 0.34	**9**	34.69 ± 0.28
2	34.66 ± 0.28	**10**	35.35 ± 0.31
3	36.44 ± 0.031	**11**	N.A.
4	59.66 ± 0.21	**12**	N.A.
5	5.45 ± 0.08	**13**	3.49 ± 0.05
6	49.54 ± 0.61	**14**	88.66 ± 1.20
7	1.26 ± 0.01	**15**	38.64 ± 0.34
8	8.66 ± 0.08	**Acarbose**	38.25 ± 0.12

SEM, standard error mean; N.A., not active.

with reference to acarbose are compounds **3**, **9** and **10**. These compounds are para-substituted with nitro, nitrile and methoxy substituents. Two compounds, **11** and **12**, are not showing any inhibition activity. Bulky and incapable of forming hydrogen bonding with residues of α-glucosidase might be the reason for the low activity of these compounds. Compound **13**, which is having two fluorine atoms substituted directing on the extended ring, is the second most active compound with an IC_{50} value of 3.49 ± 0.05 μM.

Docking study

Molecular docking studies were performed to gain insight into the most probable binding conformation of flavone ether derivatives (**3**–**15**), which in return explains the reason for their potency. Docking studies had been carried out using α-glucosidase structure obtained from homology modelling as crystal structure for α-glucosidase of *S. cerevisiae* is still not available (59). Isomaltase (EC 3.2.1.10, oligo-1,6-glucosidase, MALX3) (PDB code: 3A4A) from baker's yeast, which shares 71% identity and 84% similarity with the target enzyme, α-glucosidase of *S. cerevisiae,* had been used as the template for homology modelling. Homology modelling had been carried out using SWISS-MODEL. The RMSD value between the original protein isomaltase (PDB code: 3A4A) and the homology model is 0.169 Å. Sequence analysis on the homology model's sequence showed high sequence homology with the target enzyme with active site remains intact and highly conserved (Figure 1).

Docking method was validated by doing control docking of native inhibitor. Acarbose was docked into α-glucosidase from sugar beet (PDB code: 3W37). Comparison through superimpose of native ligand with docking results shows that docking method could reproduce the binding mode of acarbose in α-glucosidase from sugar beet (Figure 2). The rmsd value between actual and docked pose was found to be 0.65 Å. Even though α-glucosidase from sugar beet shares relatively low homology with baker's yeast α-glucosidase (16% identity), the active site is highly conserved and main interactions of the ligand remain the same (60).

Docking studies carried out on all flavone ethers (**3**–**15**) had provided us with some good results, which best explain the compounds *in vitro*. Important structural feature like ether linkage and substitution on the compounds' side chain were observed closely to further rationalize the inhibition activity. Methyloxy linkage (-CH_2-O-) increases flexibility and reduces torsional stress of the derivatives. This allows the extended ring to be placed properly within active site (Figure 3). This is supported by a study carried out by Moorthy *et al.* (61), which states that increase in flexibility of molecules will reduce stretching energy required for molecules to interact with the active site.

Other important structural feature would be the benzopyran-4-one moiety. In this study, flavone rings A and B were stabilized by interacting with backbone (ND2) of Asn347 through Pi-donor interactions. Pyrone moiety (ring B) was further stabilized through Pi-Pi stacking interaction with Phe300. On the other hand, Asp349 stabilizes ring C and extended ether portion through anion–Pi interaction

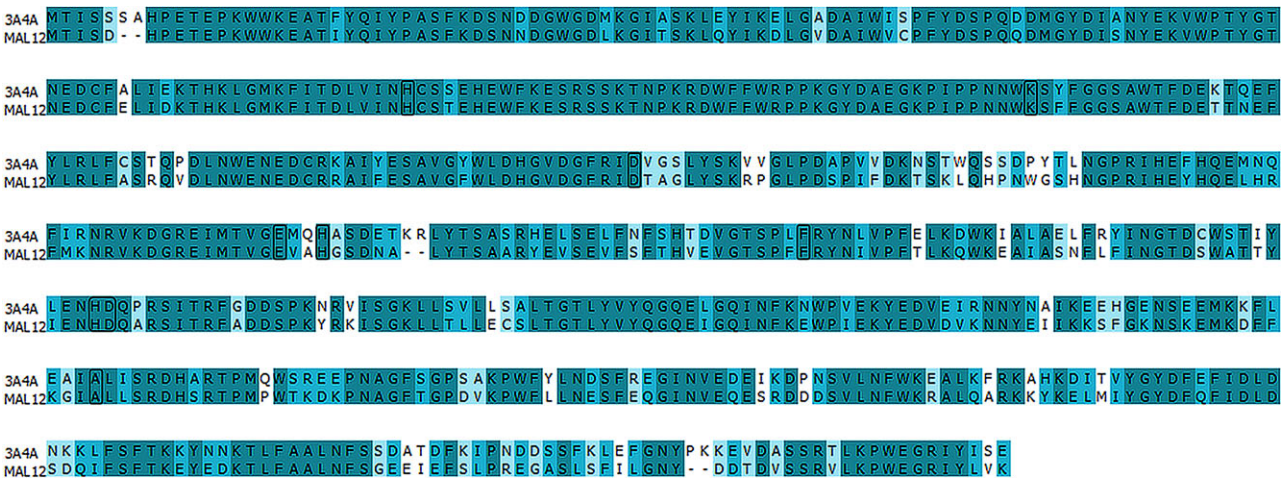

Figure 1: Comparison between sequence of homology model (3A4A) and MAL12.

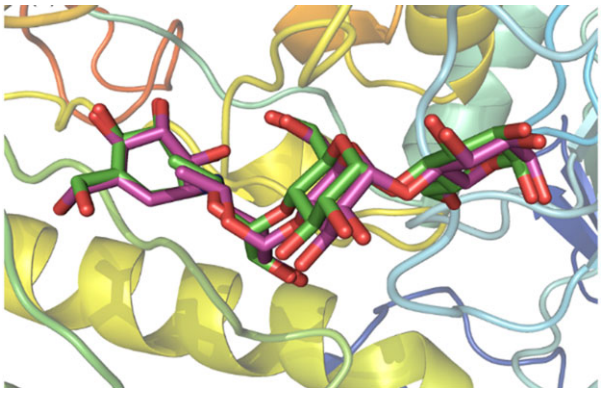

Figure 2: Superimpose of acarbose in α-glucosidase from sugar beet (3W37).

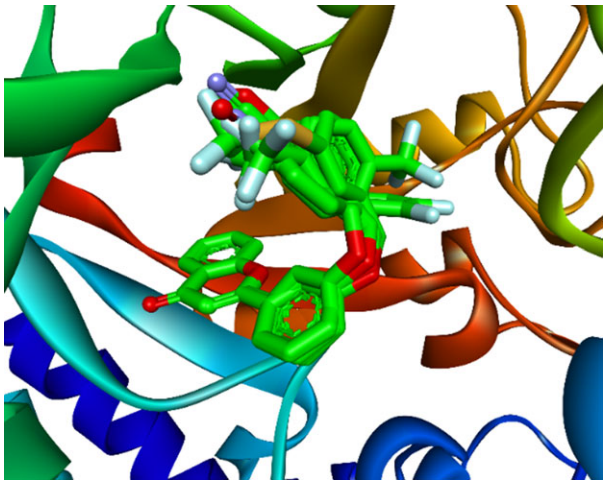

Figure 3: Active compounds aligned in the binding cavity.

between its backbone (OD1 and OD2) with both rings. Asp214 was observed to enhance stability of the extended ring through another anion–Pi interaction with its backbone (OD2). The carbonyl's oxygen of flavone ring for all active compounds acts as a hydrogen bond acceptor and forms interaction with hydroxyl group of Tyr344. Carbon–hydrogen interaction was observed between CH_2 of methyloxy linkage (-CH_2-O-) and side chain carboxyl oxygen (OD2) of Asp349.

Study on interaction of the side chain's substituents showed the importance of fluorine in the activity (Figure 4). Docking for active compounds **5** (5.45 ± 0.08 μM), **7** (1.26 ± 0.01 μM), **8** (8.66 ± 0.08 μM) and **13** (3.49 ± 0.05 μM) having activity showed how fluorine substituents influence the activity. Trifluoromethyl substituent that is a common feature for active compounds **5**, **7** and **8** are oriented towards the hydrophobic pocket made up of Phe300, Phe177, Phe157 and Ala278. The fact that fluorine has low polarizability and its ability to inhibit α-glucosidase is supported by claims that better interaction can be observed by lowering compounds polarizability properties (61–63). Fluorine atom for compound **5** forms a halogen bond was formed between one of fluorine atom with side chain carboxyl oxygen (OG2) of Thr215 (3.68 Å). Compound **7** has two trifluoromethyl substituents, positioned at C-2 and C-5 on ether's side ring. Trifluoromethyl substituent at C-2 was well positioned in hydrophilic pocket of Phe300, Phe177, Phe157 and Ala278, while the second trifluoromethyl substituent was positioned towards a hydrophilic region surrounded by Asp68, Asp214 and Tyr71. A carbon–hydrogen interaction was also observed between CH2 of flavone and side chain carboxyl oxygen (OD2) of Asp349 (3.54 Å). As for the three fluorine atoms in the hydrophilic pocket, one of the halide forms a bond with the backbone (OD2) of Asp68 (3.04 Å). The other two fluorine atoms form bondings with the Asp214 (OD1 and OD2) at the distance of 2.72 and 2.98 Å. Halide bondings with polar residues such as Asp68 and Asp214 were not observed for other compounds, especially for compounds **5** and **8** as they have the trifluoromethyl substitution. Based on docking results, trifluoromethyl substitution gives the best effect in *ortho* position as being shown by compound **7**. Trifluoromethyl substitution at *meta* position (compounds **5** and **8**) could not compensate for the steric repulsion towards the hydrophilic region. This causes the trifluoromethyl substituent to be positioned towards the hydrophobic pocket. The ability of compound **7** to interact with Tyr71 and Phe177 is extremely important. This is because Tyr71 and Phe177 are experimentally determined to be crucial for the terminal ring recognition of substrates by α-glucosidase (64).

Besides compounds having trifluoromethyl substitution, compound **11** (3.49 ± 0.05 μM), which is a 2,5-difluoro-substituted compound showed good inhibition by being second most active compound in the series. Common interactions were observed between carbonyl's oxygen of flavone ring with hydroxyl group of Tyr344 (2.47 Å). Oxygen of ether linkage forms a stable interaction with NH1 of Arg439 at a distance of 3.38 Å. It was observed that Arg439 (NH1) forms second bond with fluorine substituted at ortho position with a distance of 2.70 Å. The other fluorine atom forms interaction with backbone (OD2) of Asp68 (2.60 Å). The ligand–receptor complex was stabilized by Asp214, Phe300, Asn347 and Asp349 through some electrostatic, hydrogen bond and hydrophobic interactions.

Park *et al.* (21) claims that phenolic oxygen is able to form a two-way hydrogen bond interaction with the side chain of two residues, His348 and Asp349, believed to play a critical role in the catalytic mechanism. However, in this study, which involves no phenolic oxygen, it was observed that indirect interaction with His348 and Asp349 further stabilizes the enzyme–ligand complex. The docking results also indicate that the active compounds can be stabilized

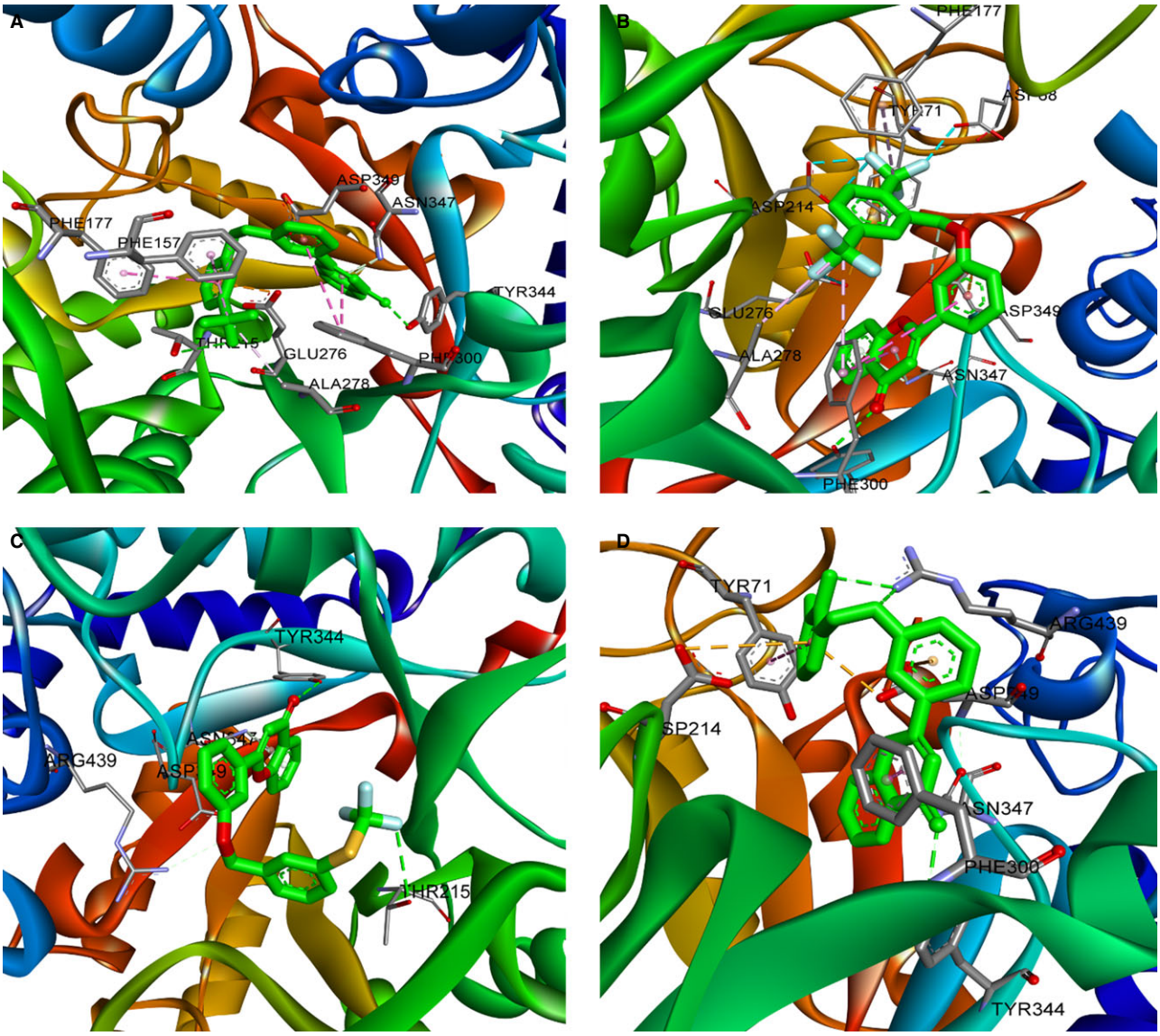

Figure 4: Binding position of active (A) compounds **5**, (B) **7**, (C) **8** and (D) **13**.

in the active site through hydrophobic interactions of chromene ring with the side chains of Phe, Ile, Trp, Met, Ala and His as being reported by Park *et al.* (21).

Observation on compounds **1**, **6**, **9** and **10** showed that their activities are influenced by the substituents on ether's side ring (Figure 5). The best docking pose showed that nitro, nitrile, *tert*-butyl and methoxy substituent at para position are well oriented towards the same hydrophobic pocket as being observed for trifluoromethyl substituent, but they are unable to form any meaningful interaction. Studies showed that nitro, nitrile and methoxy substituents are only forming hydrogen bonding with Thr215 at a distance of 3.11, 2.80 and 2.63 Å, respectively. *Tert*-butyl substituent of compound **6** is not showing any interaction with the surrounding residues. The results support claims made by Moorthy *et al.* (65) based on a QSAR study of chromanone derivatives, in which it was found that compounds having dipole moment groups and highly hydrophobic substituents could reduce α-glucosidase inhibitory activity.

Conclusion

From this study, we manage to synthesize some new derivatives of flavone ether and evaluate them for their inhibiting α-glucosidase. Better activity for compound **2** as compared to acarbose and compound **2** strongly suggests the importance of chromone moiety, especially the pyrone ring in inhibiting α-glucosidase activity. Compound **7**, which is having trifluoromethyl-substituted at positions 2

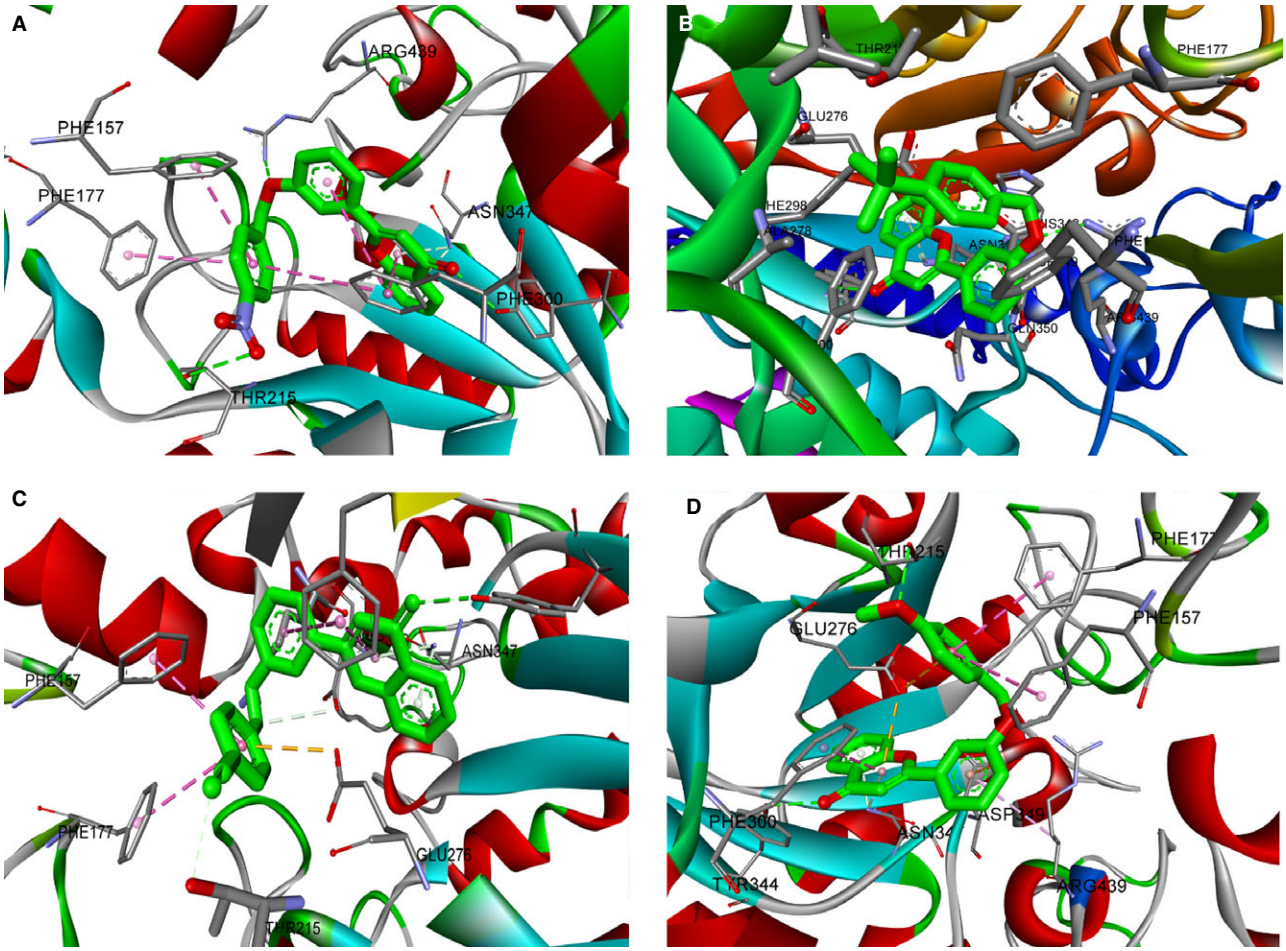

Figure 5: Docking of inactive (A) compounds **3**, (B) **6**, (C) **9** and (D) **10**.

and 5 on its ether side ring, recorded the highest inhibition activity with an IC_{50} value of 1.26 ± 0.01 μM. Trifluoromethyl substituent at position 2 was well positioned in hydrophilic pocket of Phe300, Phe177, Phe157 and Ala278. The second trifluoromethyl substituent was position towards a hydrophilic region surrounded by Asp68, Asp214 and Tyr71. A carbon–hydrogen interaction was also observed between CH2 of flavone and side chain carboxyl oxygen (OD2) of Asp349 (3.54 Å). As for the three fluorine atoms in the hydrophilic pocket, one of the halides forms a bond with the backbone (OD2) of Asp68 (3.04 Å). The other two fluorine atoms form bondings with the Asp214 (OD1 and OD2) at the distance of 2.72 and 2.98 Å. Halide bondings with polar residues such as Asp68 and Asp214 were not observed for other compounds, especially for compounds **5** and **8** as they have the trifluoromethyl substitution. Besides being able to interact with one of the most important residues Asp214, the ability of compound **7** to interact with Tyr71 and Phe177 should be significantly considered. This is because Tyr71 and Phe177 play an important role in terminal ring recognition of substrates by α-glucosidase and this may have contributed in the inhibition activity.

Acknowledgments

The authors would like to acknowledge Universiti Teknologi MARA for the financial support through research grant, UiTM 100-RMI/MOA 16/6/2 (1/2013). The first author would like to thank Ministry of Higher Education Malaysia for the financial funding through MyBrain15 scholarship.

References

1. Lim E.L., Hollingsworth K.G., Aribisala B.S., Chen M.J., Mathers J.C., Taylor R. (2011) Reversal of type 2 diabetes: normalisation of beta cell function in association with decreased pancreas and liver triacylglycerol. Diabetologia;54:2506–2514.
2. Bisht S., Kant R., Kumar V. (2013) α-d-Glucosidase inhibitory activity of polysaccharide isolated from Acacia tortilis gum exudate. Int J Biol Macromol;59:214–220.
3. Hu X.J., Wang X.B., Kong L.Y. (2013) α-Glucosidase inhibitors via green pathway: biotransformation for

bicoumarins catalyzed by *Momordica charantia* Peroxidase. J Agric Food Chem;61:1501.
4. Chen Y.-G., Li P., Li P., Yan R., Zhang X.-Q., Wang Y., Zhang X.-T., Ye W.-C., Zhang Q.-W. (2013) α-Glucosidase inhibitory effect and simultaneous quantification of three major flavonoid glycosides in *Microctis folium*. Molecules;18:4221–4232.
5. Danaei G., Finucane M.M., Lu Y., Singh G.M., Cowan M.J., Paciorek C.J., Lin J.K., Farzadfar F., Khang Y.-H., Stevens G.A., Rao M., Ali M.K., Riley L.M., Robinson C.A., Ezzati M. (2011) National, regional, and global trends in fasting plasma glucose and diabetes prevalence since 1980: systematic analysis of health examination surveys and epidemiological studies with 370 country-years and 2.7 million participants. Lancet;378:31–40.
6. Whiting D.R., Guariguata L., Weil C., Shaw J. (2011) IDF diabetes atlas: global estimates of the prevalence of diabetes for 2011 and 2030. Diabetes Res Clin Pract;94:311–321.
7. Mathers C.D., Loncar D. (2006) Projections of global mortality and burden of disease from 2002 to 2030. PLoS Med;3:e442.
8. Taylor S.I., Accili D., Imai Y. (1994) Insulin resistance or insulin deficiency: which is the primary cause of NIDDM? Diabetes;43:735–740.
9. Porte D. Jr (1991) β-cells in type II diabetes mellitus. Diabetes;40:166–180.
10. Butler A.E., Janson J., Bonner-Weir S., Ritzel R., Rizza R.A., Butler P.C. (2003) β-cell deficit and increased β-cell apoptosis in humans with type 2 diabetes. Diabetes;52:102–110.
11. Tang P.C., Lin Z.G., Wang Y., Yang F.L., Wang Q., Fu J.H., Zhang L., Gong A.S., Luo J.J., Dai J., She G.H., Si D.D., Feng J. (2010) Design and synthesis of DPP-4 inhibitor for the treatment of type 2 diabetes. Chin Chem Lett;21:253–256.
12. Wu Y.H. (2007) Synthesis of (S)-2-ethoxy-3-phenylpropanoic acid derivatives and their insulin-sensitizing activity. Chin J Chem;25:265–267.
13. Wang Y.F., Yang Z.W., Wei X.L. (2010) Sugar compositions, α-glucosidase inhibitory and amylase inhibitory activities of polysaccharides from leaves and flowers of *Camellia sinensis* obtained by different extraction methods. Int J Biol Macromol;47:534–539.
14. Puls W., Keup U., Krause H.P., Thomas G., Hoffiester F. (1977) Glucosidase inhibition. Naturwissenschaften;64:536–537.
15. Shim Y.J., Doo H.K., Ahn S.Y., Kim Y.S., Seong J.K., Park I.S., Kim B.H. (2003) Inhibitory effect of aqueous extract from the gall of *Rhus chinensis* on alpha-glucosidase activity and postprandial blood glucose. J Ethnopharmacol;85:283–287.
16. Samad A.H., Willing T.S.T., Alberti K.G.M., Taylor R. (1988) Effects of BAYm 1099, new α-glucosidase inhibitor, on acute metabolic responses and metabolic control in NIDDM over 1 mo. Diabetes Care;11:337–344.
17. O'Dea K., Turton J. (1985) Optimum effectiveness of intestinal alpha-glucosidase inhibitors: importance of uniform distribution through a meal. Am J Clin Nutr;41:511–516.
18. Asano N. (2003) Glycosidase inhibitors: update and perspectives on practical use. Glycobiology;13:93R–104R.
19. Charron M.J., Dubin R.A., Michels C.A. (1986) Structural and functional analysis of the MAL1 locus of *Saccharomyces cerevisiae*. Mol Cell Biol;6:3891–3899.
20. Humphries M.J., Matsumoto K., White S.L., Olden K. (1986) Inhibition of experimental metastasis by castanospermine in mice: blockage of two distinct stages of tumor colonization by oligosaccharide processing inhibitors. Cancer Res;46:5215–5222.
21. Park H., Hwang K.Y., Oh K.H., Kim Y.H., Lee J.Y., Kim K. (2008) Discovery of novel α-glucosidase inhibitors based on the virtual screening with the homology-modeled protein structure. Bioorg Med Chem;16:284–292.
22. Storr S.J., Royle L., Chapman C.J., Hamid U.M.A., Robertson J.F., Murray A., Dwek R.A., Rudd P.M. (2008) The O-linked glycosylation of secretory/shed MUC1 from an advanced breast cancer patient's serum. Glycobiology;18:456–462.
23. De Melo E.B., da Silveira G.A., Carvalho I. (2006) α- and β-Glucosidase inhibitors: chemical structure and biological activity. Tetrahedron;62:10277–10302.
24. Gamblin D.P., Scanlan E.M., Davis B.G. (2008) Glycoprotein synthesis: an update. Chem Rev;109:131–163.
25. Park H., Hwang K.Y., Kim Y.H., Oh K.H., Lee J.Y., Kim K. (2008) Discovery and biological evaluation of novel α-glucosidase inhibitors with *in vivo* antidiabetic effect. Bioorg Med Chem Lett;18:3711–3715.
26. Rawlings A.J., Lomas H., Pilling A.W., Lee M.J.R., Alonzi D.S., Rountree J., Jenkinson S.F., Fleet G.W.J., Dwek R.A., Jones J.H., Butters T.D. (2009) Synthesis and biological characterisation of novel N-Alkyl-deoxynojirimycin α-glucosidase inhibitors. Chem Bio Chem;10:1101–1105.
27. Sunkara P.S., Kang M.S., Bowlin T.L., Liu P.S., Tyms A.S., Sjoerdsma A. (1990) Inhibition of glycoprotein processing and HIV replication by castanospermine analogues. Ann N Y Acad Sci;616:90–96.
28. Dennis J.W., Waghorne S.L.C., Breitman M.L., Kerbel R.S. (1987) Beta 1-6 branching of Asn-linked oligosaccharides is directly associated with metastasis. Science;236:582–585.
29. Durinx C., Lambeir A.M., Bosmans E., Falmagne J.B., Berghmans R., Haemers A., Scharpé S., De Meester I. (2000) Molecular characterization of dipeptidyl peptidase activity in serum. Eur J Biochem;267:5608–5613.
30. Lee D., Woo J.K., Kim D., Kim M., Cho S.K., Kim J.H., Park S.P., Lee H.Y., Riu K.Z., Lee D.-S. (2011) Antiviral activity of methylelaiophylin, an α-glucosidase inhibitor. J Microbiol Biotech;21:263–266.
31. Jacob G.S. (1995) Glycosylation inhibitors in biology and medicine. Curr Opin Struct Biol;5:605–611.

32. Simsek E., Lu X., Ouzounov S., Block T.M., Mehta A.S. (2006) α-Glucosidase inhibitors have a prolonged antiviral effect against hepatitis B virus through the sustained inhibition of the large and middle envelope glycoproteins. Antivir Chem Chemother;17:259–267.
33. Singh M., Kaur M., Silakari O. (2014) Flavones: an important scaffold for medicinal chemistry. Eur J Med Chem;84:206–239.
34. Xu J.D., Zhang L.W., Liu Y.F. (2013) Synthesis and antioxidant activities of flavonoids derivatives, troxerutin and 3′, 4′, 7-triacetoxyethoxyquercetin. Chin Chem Lett;24:223–226.
35. Zheng J.B., Zhang H.F., Gao H. (2005) Investigation on electrochemical behavior and scavenging superoxide anion ability of chrysin at mercury electrode. Chin J Chem;23:1042–1046.
36. Ly H.D., Withers S.G. (1999) Mutagenesis of glycosidases. Ann Rev Biochem;68:487–522.
37. Schewe T., Steffen Y., Sies H. (2008) How do dietary flavanols improve vascular function? A position paper. Arch Biochem Biophysics;476:102–106.
38. Clifford M.N. (1999) Chlorogenic acids and other cinnamates–nature, occurrence and dietary burden. J Sci Food Agric;79:362–372.
39. Richelle M., Tavazzi I., Offord E. (2001) Comparison of the antioxidant activity of commonly consumed polyphenolic beverages (coffee, cocoa, and tea) prepared per cup serving. J Agric Food Chem;49:3438–3442.
40. Crozier A., Jaganath I.B., Clifford M.N. (2009) Dietary phenolics: chemistry, bioavailability and effects on health. Nat Prod Rep;26:1001–1043.
41. Wang Q.Q., Cheng N., Zheng X.W., Peng S.M., Zou X.Q. (2013) Synthesis of organic nitrates of luteolin as a novel class of potent aldose reductase inhibitors. Bioorg Med Chem;21:4301–4310.
42. Cui J.H., Hu D., Zhang X., Jing Z., Ding J., Wang R.-B., Li S.-S. (2013) Design and synthesis of new 7, 8-dimethoxy-α-naphthoflavones as CYP1A1 inhibitors. Chin Chem Lett;24:215–218.
43. Nishioka T., Kawabata J., Aoyama Y. (1998) Baicalein, an α-glucosidase inhibitor from *Scutellaria baicalensis*. J Nat Prod;61:1413–1415.
44. Sak K. (2014) Cytotoxicity of dietary flavonoids on different human cancer types. Pharmacogn Rev;8:122.
45. Shin J.S., Kim K.S., Kim M.B., Jeong J.H., Kim B.K. (1999) Synthesis and hypoglycemic effect of chrysin derivatives. Bioorg Med Chem Lett;9:869–874.
46. Taha M., Ismail N.H., Lalani S., Fatmi M.Q., Siddiqui S., Khan K.M., Imran S., Choudhary M.I. (2015) Synthesis of novel inhibitors of α-glucosidase based on the benzothiazole skeleton containing benzohydrazide moiety and their molecular docking studies. Eur J Med Chem;92:387–400.
47. Taha M., Ismail N.H., Imran S., Rokei M.Q.B., Saad S.M., Khan K.M. (2015) Synthesis of new oxadiazole derivatives as α-glucosidase inhibitors. Bioorg Med Chem;23:4155–4162.
48. Khan K.M., Rahim F., Wadood A., Kosar N., Taha M., Lalani S., Khan A., Fakhri M.I., Junaid M., Rehman W., Khan M., Perveen S., Sajid M., Choudhary M.I. (2014) Synthesis and molecular docking studies of potent α-glucosidase inhibitors based on biscoumarin skeleton. Eur J Med Chem;81:245–252.
49. Rahim F., Ullah K., Ullah H., Wadood A., Taha M., Rehman A.U., Uddin I., Ashraf M., Shaukat A., Rehman W., Hussain S., Khan K.M. (2015) Triazinoindole analogs as potent inhibitors of α-glucosidase: synthesis, biological evaluation and molecular docking studies. Bioorg Chem;58:81–87.
50. Taha M., Ismail N.H., Baharudin M.S., Lalani S., Mehboob S., Khan K.M., Siddiqui S., Rahim F., Choudhary M.I. (2015) Synthesis crystal structure of 2-methoxybenzoylhydrazones and evaluation of their α-glucosidase and urease inhibition potential. Med Chem Res;24:1310–1324.
51. Kiefer F., Arnold K., Kunzli M., Bordoli L., Schwede T. (2009) The SWISS-MODEL repository and associated resources. Nucleic Acids Res;37:D387–D392.
52. Arnold K., Bordoli L., Kopp J., Schwede T. (2006) The SWISS-MODEL workspace: a web-based environment for protein structure homology modelling. Bioinformatics;22:195–201.
53. Guek N., Peitsch M.C., Schwede T. (2009) Automated comparative protein structure modeling with SWISS-MODEL and Swiss-PdbViewer: a historical perspective. Electrophoresis;30(Suppl. 1):S162–S173.
54. Morris G.M., Huey R., Lindstrom W., Sanner M.F., Belew R.K., Goodsell D.S., Olson A.J. (2009) AutoDock4 and AutoDockTools4: automated docking with selective receptor flexibility. J Comp Chem;30:2785–2791.
55. Taha M., Ismail N.H., Jamil W., Rashwan H., Kashif S.M., Sain A.A., Adenan M.I., Anouar E.H., Ali M., Rahim F., Khan K.M. (2014) Synthesis of novel derivatives of 4-methylbenzimidazole and evaluation of their biological activities. Eur J Med Chem;84:731–738.
56. Saify Z.S., Kamil A., Akhtar S., Taha M., Khan A., Khan K.M., Jahan S., Rahim F., Perveen S., Choudhary M.I. (2014) 2-(2′-Pyridyl) benzimidazole derivatives and their urease inhibitory activity. Med Chem Res;23:4447–4454.
57. Taha M., Ismail N.H., Imran S., Selvaraj M., Rashwan H., Farhanah F.U., Rahim F., Kesavanarayanan K.S., Ali M. (2015) Synthesis of benzimidazole derivatives as potent β-glucuronidase inhibitors. (2015). Synthesis of benzimidazole derivatives as potent β-glucuronidase inhibitors. Bioorg Chem;61:36–44.
58. Imran S., Taha M., Ismail N.H., Fayyaz S., Khan K.M., Choudhary M.I. (2015) Synthesis, biological evaluation, and docking studies of novel thiourea derivatives of bisindolylmethane as carbonic anhydrase II inhibitor. Bioorg Chem;62:83–93.
59. Barakat A., Soliman S.M., Al-Majid A.M., Lotfy G., Ghabbour H.A., Fun H.K., Yousuf S., Choudhary M.I., Wadood A. (2015) Synthesis and structure investiga-

tion of novel pyrimidine-2, 4, 6-trione derivatives of highly potential biological activity as anti-diabetic agent. J Mol Struct;1098:365–376.
60. Yar M., Bajda M., Shahzadi L., Shahzad S.A., Ahmed M., Ashraf M., Alam U., Khan I.U., Khan A.F. (2014) Novel synthesis of dihydropyrimidines for α-glucosidase inhibition to treat type 2 diabetes: *in vitro* biological evaluation and *in silico* docking. Bioorg Chem;54:96–104.
61. Moorthy N.S., Ramos M.J., Fernandes P.A. (2012) Structural analysis of structurally diverse α-glucosidase inhibitors for active site feature analysis. J Enz Inhib Med Chem;27:649–657.
62. Moorthy N.S., Ramos M.J., Fernandes P.A. (2012) Studies on α-glucosidase inhibitors development: magic molecules for the treatment of carbohydrate mediated diseases. Mini Rev Med Chem;12:713–720.
63. Silva C.H.T.P., Taft C.A. (2004) Computer-aided molecular design of novel glucosidase inhibitors for AIDS treatment. J Biomol Struct Dyn;22:59–63.
64. Roujeinikova A., Raasch C., Sedelnikova S., Liebl W., Rice D.W. (2002) Crystal structure of *Thermotoga maritima* 4-α-glucanotransferase and its acarbose complex: implications for substrate specificity and catalysis. J Mol Biol;321:149–162.
65. Moorthy N.S., Ramos M.J., Fernandes P.A. (2011) Analysis of the α-glucosidase inhibitory activity of chromenone derivatives based on their molecular features: a computational study. Med Chem;7:526–533.

Notes

[a]Accelrys Software Inc., Discovery Studio Modeling Environment, Release 3.5, San Diego: Accelrys Software Inc.
[b]The PyMol Molecular Graphics System, Version 1.1 Schrödinger, LLC.

Supporting Information

Additional Supporting Information may be found in the online version of this article:

Appendix S1. Proton NMR for flavone ether 1-15.